Proceedings of the
9th Graz Brain-Computer Interface Conference 2024
10.3217/978-3-99161-014-4-063

AN ALTERNATIVE TRAINING PROTOCOL FOR A MOTOR IMAGERY BMI BASED ON A COLLABORATIVE APPROACH

Alessio Palatella[1], Paolo Forin[1], Stefano Tortora[1,2], Emanuele Menegatti[1,2], Luca Tonin[1,2]

[1]Department of Information Engineering, University of Padova, Padova, Italy
[2]Padova Neuroscience Center, University of Padova, Padova, Italy

E-mail: stefano.tortora@unipd.it

ABSTRACT: Becoming proficient in the use of brain-machine interfaces (BMIs) represents a challenging task for the subjects, requiring long and intensive training. In this paper, we propose and explore the use of a collaborative BMI (cBMI) as an innovative training protocol that allows two subjects to learn together by cooperating in the control of a real robotic arm. Preliminary results on three pairs of subjects spanning five days of training highlight the promises of the proposed approach in reducing the training time and possibly mitigating the frustration in naive users.

INTRODUCTION

Motor imagery (MI) brain-machine interfaces (BMIs) represent the most natural approach to control brain-driven robotic devices [1]. Indeed, the endogenous paradigm used in BMIs provides the advantage that subjects can autonomously initiate mental tasks without requiring external stimuli like visual, auditory, or tactile cues, making the interaction with the robotic system more natural [2].

However, becoming proficient using MI BMIs is a challenging scenario that requires a substantial investment of time and effort for the subject [3]. In the last years, researchers have shown that training directly on the final application might be more effective than having subjects engaged in repetitive and artificial mental tasks [4, 5]. However, this approach may not always be practical for naive subjects, given the inherent limitations in the accuracy of their BMIs and the consequent frustration caused by their low performances to perform the given task. This is often attributed to their limited experience, causing them to struggle in effectively generating effective control commands [6].

In this scenario, researchers have recently proposed collaborative brain-machine interfaces (cBMIs) to deal with such limited performance [7, 8]. In this approach, multiple subjects are simultaneously engaged in the same BMI task and the output of their BMIs is combined to enhance the decoding accuracy or increase the number of commands.

One crucial aspect of cBMIs is how the data originating from multiple sources is integrated to generate a single control signal. In the literature, two main approaches are reported: on the one hand, researchers investigated the possibility to merge the sources at the feature level and then to exploit this unified signal to train a single decoder [9, 10]. On the other hand, it has been explored the feasibility to train a decoder for each subject, and then to combine the output at the decision level to obtain the final command for the external device [7, 8, 11].

In literature, cBMI are typically employed in experiments with BMI based on exogenous visual stimulation or pattern recognition. In a study by Wang et al. [11], 15 subjects were divided into subgroups and they performed animal categorization and single-photograph recognition with a Go/noGo paradigm through a series of flashing pictures. Similarly, Poli et al. [7] instructed 10 subjects to determine whether two subsequent shapes, with the second one masked, were identical and pressing a button consequently. In another study by Valeriani et al. [9], participants were asked to identify the specific geometrical patterns of two horizontal and vertical bars to use a switch to send the decisions.

To date, research on cBMI with MI BMI is limited, and the studies that apply this concept to control a robot in real-life scenarios are neglected. For instance, Yijie et al. [10] independently trained eight subjects in hands and feet motor imagery for moving a point on a grid. They combined the individual subjects' results offline to simulate a collaborative protocol. In a different study, Bonnet et al. [8] developed a game where subject pairs control the movement of a virtual ball using motor imagery, both collaboratively and competitively, to place it inside a net. The game software uses the two decoders' output to decide in which direction the ball should move and change the feedback accordingly. However, the literature predominantly emphasizes subject performance and methods to enhance classification accuracy, and there are no studies reporting on the subject's learning during cBMI.

In this work, we aim to investigate this particular aspect by exploring the cBMI as a novel approach to assist subjects during the training of MI BMI. Our training protocol grounded on the concept that when we learn complex skills in our daily life (e.g., cycling, driving), we are not alone. Based on this, we have designed an alternative training protocol utilizing a cBMI where two subjects work together to accomplish the same task of controlling a robotic arm during reaching operations. The rationale

Published by
Verlag der Technischen Universität Graz

10.3217/978-3-99161-014-4-063

is that the presence of a second subject can help the less proficient one to still conclude the task, decreasing negative mental states due to frustration or inefficiency present in other BMI [12]. We hypothesize that this approach can increase overall performance and promote learning in both subjects [13].
The objective of this work is twofold: firstly, to showcase the viability of MI cBMI for controlling a real robotic device even in the early stage of the training; secondly, to investigate this collaborative approach as a promoter of individual learning of BMI skills.

METHODS

Participants: Six healthy subjects, with an average age of 25±2 years, were recruited and divided into three pairs (G1-C7, G2-D7, C9-C8). Moreover, three of them had no experience with BMI system before (G1, G2, C9). The first three sessions took place over two weeks in December 2023, while the remaining three sessions were conducted over three weeks in January 2024. Each participant provided consent by signing a form detailing the use of recorded data and privacy protocols, adhering to the principles outlined in the Declaration of Helsinki.

Experimental design: The experiment comprised six sessions, each consisting of three runs, as illustrated in Figure 1a. The initial session (Session - Day 0) involved the calibration and evaluation of the BMI Gaussian decoder of each subject. The following sessions (Session - Day 1-5) focused on online runs, during which subjects tested the trained decoder, re-training it if its accuracy where below 70% [14] with two new calibrations and evaluations, and subsequently controlled the robotic arm in collaboration with another subject. All sessions are subdivided into runs, which can be of three types: calibration runs for recording the data for training the decoder; evaluation runs to test the decoder performance; control runs where subjects controlled the robotic arm using the proposed cBMI.
During the control runs, subjects were asked to move a robotic arm from a home position to one of the five target objects placed on a circle of radius 50 cm in front of the robot. Subjects were allowed to see the robot and the workspace on a monitor, with superimposed visual feedback as depicted in Figure 1b. At the beginning of each trial, subjects were presented with a target object to pick, indicated by a blue dot, for 1 s (cue period). After that, the robot initiated the motion based on the output of the cBMI. When sufficiently close to an object, the robot autonomously performed the pick, returned in the home position, and a new trial started. For each run, subjects were required to pick each of the five objects twice, hence ten trials in total. Figure 1 (c) shows the experimental setup, comprising the subjects, the robotic arm, and monitors for visual feedback. The combination of the brain-machine interfaces (BMIs) output is also provided as visual feedback using a rotating wheel[1].

[1]Video: https://cloud.dei.unipd.it/index.php/s/TgYJ475A9M7tz3x

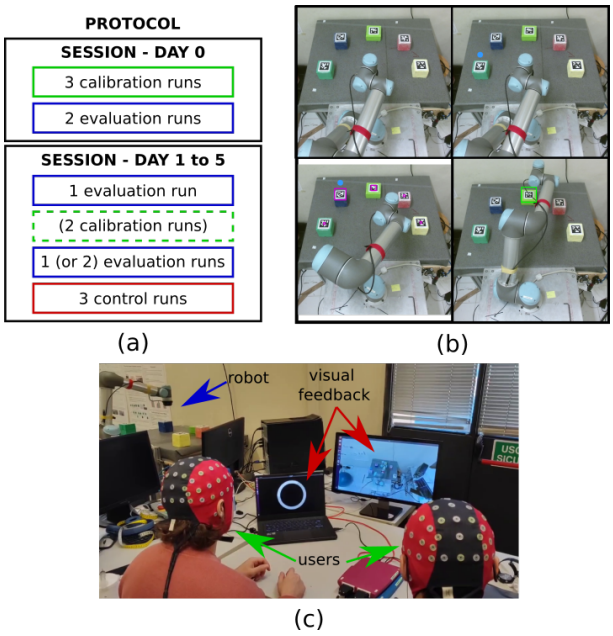

Figure 1: Experimental design. (a) Schematic representation of the experiment division for sessions (days). (b) BMI visual feedback provided to the subject to control the robotic arm. (c) Experimental set-up for the controlling runs in which both subjects controlled the manipulator.

Collaborative BMI: We acquired electroencephalography (EEG) data with a 64-channel amplifier (AntNeuro eego sports 64, Netherlands) operating at a sampling rate of 512 Hz. A 2-class MI paradigm was employed where the subjects were required to make the kinesthetic imagination of their feet or their hands. Our method was based on a classical MI BMI already widely evaluated in literature [6, 15]. In particular, we selected a subset of 32 electrodes placed over the sensorimotor cortex (i.e., $FP1$, $FP2$, FZ, $FC5$, $FC1$, $FC2$, $FC6$, $C3$, CZ, $C4$, $CP5$, $CP1$, $CP2$, $CP6$, $P3$, P_z, $P4$, $F1$, $F2$, $FC3$, FCZ, $FC4$, $C5$, $C1$, $C2$, $C6$, $CP3$, $CP4$, $P5$, $P1$, $P2$, $P6$) to detect the neural patterns related to MI. We used the power spectral density of the EEG signals with Welch's periodogram (from 4 to 48 Hz every 2 Hz) in 1-second windows sliding every 62.5 ms. The most discriminant features of each subject were identified using Canonical Variate Analysis (CVA) and a Gaussian classifier was trained with these features. The classifiers were trained on EEG data acquired during calibration or evaluation runs. During each calibration run, the subject was asked to perform 10 trials of both hands imagination, 10 trials of both feet, and trials of rest, providing always a positive feedback with the visual interface. During the evaluation, the feedback was controlled by the BMI output and the subject was asked to perform 10 trials of each MI class.

During the robot control, the output of the BMIs decoder of each subject in the pair was fused to allow the collaborative control of the robotic system. To merge the information coming from the two decoders, we applied a weighted mean on the posterior probabilities:

Published by
Verlag der Technischen Universität Graz

10.3217/978-3-99161-014-4-063

$$pp_{merged} = \frac{W_1 \cdot pp_{s_1} + W_2 \cdot pp_{s_2}}{W_1 + W_2} \quad (1)$$

The weights W_1 and W_2 were used to balance the contribution of each subject to the control according to their performance during the last evaluation run before starting the control. The weights have been computed using the balanced binary focal cross-entropy loss [16]. In particular, the weight for the subject s is obtained as $W_s = -1/L_s$ with L_s calculated as follow

$$L_s = \sum_{Tr=1}^{N} \sum_{n=1}^{N_{Tr}} \begin{cases} \frac{pp(y_n)^{\gamma} \cdot log(1-pp(y_n))}{N_{Tr}} & y_n \in class(0) \\ \\ \frac{(1-pp(y_n))^{\gamma} \cdot log(pp(y_n))}{N_{Tr}} & y_n \in class(1) \end{cases} \quad (2)$$

where N is the number of trials in the evaluation run, N_{Tr} is the number of samples in each trial and $pp(y_n)$ is the posterior probability of the decoder given the features y_n. We fixed $\gamma = 2$ as focal factor which is used to reduce the impact on the loss of well-classified samples for which $pp(y \in class(0)) < 0.6$ or $pp(y \in class(1)) > 0.4$. Finally, after the fusion process, the merged probability were integrated over time using an exponential smoothing function as $D_t = \beta \cdot D_{t-1} + (1-\beta) \cdot pp_{merged}$, where D_t and D_{t-1} are the current and previous cBMI output, respectively, and $\beta = 0.96$ is the integration coefficient.

Robot control: The commands in output from the collaborative BMI were used as input for the robotic manipulator. To this end, the integrated cBMI output D_t was mapped to an angular direction $d_R \in \{-90°, 90°\}$, with $0°$ corresponding to the forward direction, for the movement of the manipulator on the horizontal plane through the following sigmoid functions [17]:

$$d_R(D_t) = \begin{cases} -90° + \frac{90°}{1+exp(-25*(D_t-\beta_1))} & 0 \leq D_t \leq 0.5 \\ \\ \frac{90°}{1+exp(-25*(D_t-\beta_2))} & 0.5 \leq D_t \leq 1 \end{cases} \quad (3)$$

Parameters β_1 and β_2 denote the probability values at which the sigmoid intersects $-45°$ and $45°$, respectively. These parameters were initialized respectively to 0.25 and 0.75 in the first session, and then tailored to each pair at the beginning of the control runs based on the performance obtained in the previous session [17]. Given the movement direction, a velocity command was thus delivered towards that direction with constant speed equal to 5 cm/s.

In order to assist subjects in driving the robotic manipulator towards one of the target objects, the robot was controlled using a shared control architecture for teleoperation based on artificial potential fields (APF) presented in [18]. In short, the system firstly computed the probability of each target object to be the goal of the reaching task from the sequence of input velocity commands and robot positions. Then, an attractor point for the APF was generated at each time step as the center of mass of the objects' position weighted by their probability:

$$[x,y] = \sum_{n=1}^{n_{targets}} P_{(x,y)_n} \cdot p_n \quad (4)$$

where $[x,y]$ are the coordinates of the attractor point on the table surface, $P_{(x,y)_n}$ represents the position of the target n, and p_n is the probability associated to that target as computed by the shared control system. The probability of each object was also shown in real-time to the subjects through the visual feedback to help them understanding the behavior of the robotic device. For more details on the shared control implementation, please refer to [17, 18].

RESULTS

Feature evolution: Figures 2a-b summarize the evolution of the features, the distribution of the posterior probabilities and the performances of the subjects during the 5-day sessions. In particular, Figure 2b illustrates the distributions of the posterior probabilities for a pair of subjects (G1 on the x-axis and C7 on the y-axis) during the control of the robotic manipulator. It can be seen that, while subject C7 was able to span the whole range of probabilities since the first session, the second subject G1 started from a distribution quite shrank around 0.5, meaning that he was not significantly contributing to turning the robot left-right. Nevertheless, thanks to the training also subject G1 was able to expand the distribution of probabilities covering nearly the entire probability space, particularly around the extreme values during the last session. This improvement is then reflected in the distribution of the fused probabilities (Figure 2b, bottom right), where each curve colour corresponds to the same session in the scatter plots. Initially, on the first day, they were concentrated around 35% and, as sessions progressed, the distribution gradually transformed into a more uniform distribution, encompassing a broader range of possible velocity commands to control the robot. To better understand how this improvement is reflected at the neural level, we analysed the feature maps of each subject during robot control. In order to provide a reliable label (both hands or both feet) to each sample, we calculated the angle $\varphi_{ee-goal}$ between the current position of the robot's end-effector and the position of the trial's goal with respect to the forward direction. If $\varphi_{ee-goal} \geq 30°$, the corresponding EEG sample was labelled as both feet, if $\varphi_{ee-goal} \leq -30°$ as both hands, otherwise it was not considered for the feature maps analysis. Figure 2a shows for each session the grand-average across all subjects of the feature maps in the α $(8-12Hz)$ and β $(18-22Hz)$ bands calculated using the Fisher's score [4]. Overall, it can be noted a clear emergence of discriminant features through the sessions, particularly in lateral channels $(C4, C6, FC6, FC4$ and $C3, C5, FC5, FC3)$ and in the β band, as expected from our MI paradigm.

BMI accuracy: Figure 2c shows the average accuracy and the pick error for each pair over the five days. The pick accuracy is computed by counting the correct trials

Published by
Verlag der Technischen Universität Graz

10.3217/978-3-99161-014-4-063

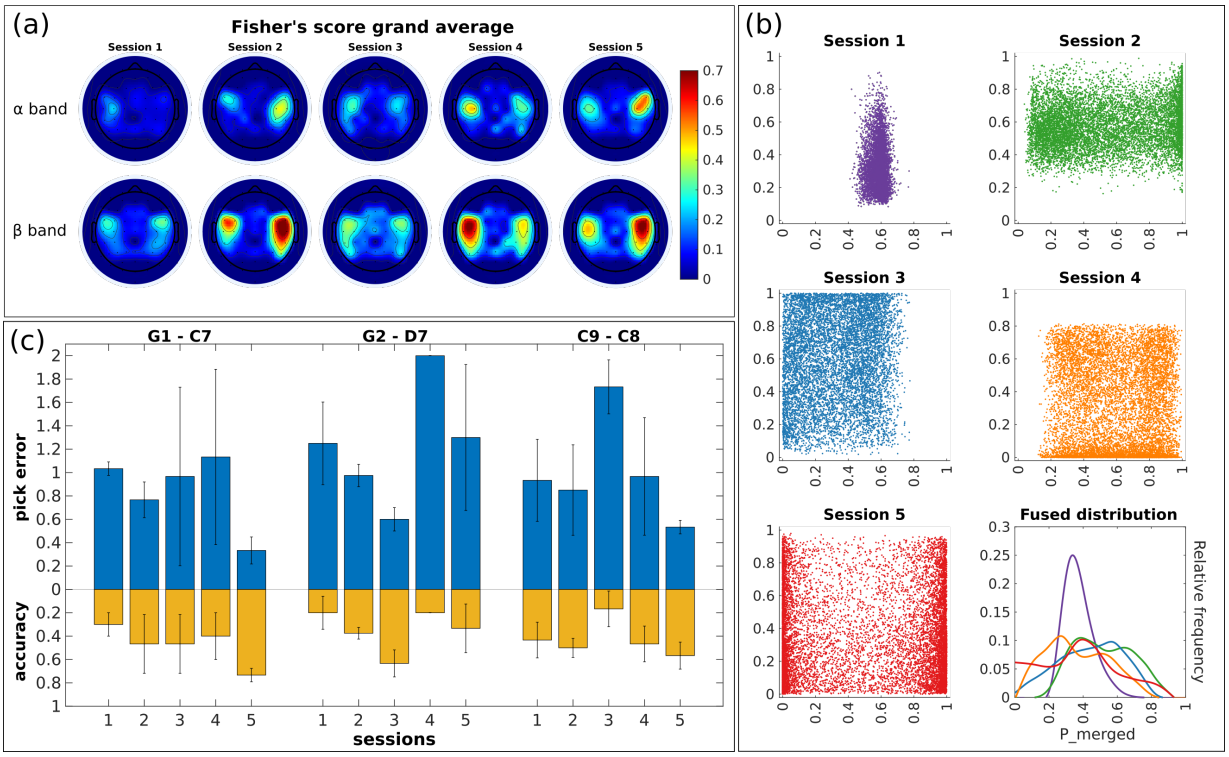

Figure 2: BMI performances. (a) Topographic representations across sessions of the grand-average feature maps of all the subjects computed as the Fischer's score in the α $(8-12Hz)$ and β $(18-22Hz)$ bands. (b) Scatter plot of the combined posterior probabilities of the pair G1-C7 during the control runs of every session (G1 on the x-axis and C7 on the y-axis). The bottom-right plot represents the distributions of the merged probabilities across the training sessions (same color as the corresponding scatter plot). (c) Pick accuracy and pick error for every pair of subjects across the five sessions.

	Robot pick accuracy [%]					Robot pick error [number of objects]				
Session	1	2	3	4	5	1	2	3	4	5
G1-C7	30 ± 10	47 ± 25	47 ± 25	40 ± 20	73 ± 5	1.0 ± 0.1	0.7 ± 0.1	0.9 ± 0.7	1.1 ± 0.7	0.3 ± 0.1
G2-D7	20 ± 14	37 ± 5	63 ± 11	20 ± 0	33 ± 20	1.2 ± 0.3	0.9 ± 0.1	0.6 ± 0.1	2.0 ± 0.0	1.3 ± 0.6
C9-C8	43 ± 15	50 ± 8	17 ± 15	46 ± 15	57 ± 11	0.9 ± 0.3	0.8 ± 0.3	1.7 ± 0.2	0.9 ± 0.5	0.5 ± 0.1

Table 1: Average pick accuracy (chance level at 20%) and pick error over the sessions for every pair.

(i.e., trials in which the manipulator reaches the correct object) over all trials. Instead, the pick error measures the precision of the control as the number of objects between the picked object and the correct one. For example, if the correct object is the one in the forward-left direction and the users pick the forward object, this error is equal to 1. On the other hand, if they pick the right-most object, the error is equal to 3. If a trial is correct, the error is equal to 0 for this trial. This metric is then normalized by the total number of trials in a single session. The average values of accuracy and pick error for each pair and each session are reported in Table 1.

Overall, all the pairs showed an improvement in performance from the first to the last session, both in terms of pick accuracy and error. The best improvement is shown by the pair G1-C7 with an increase of accuracy from 30% on average to more the 70% in the last session. Moreover, in the last session, the wrong picks are limited only to adjacent objects as highlighted by the average pick error of 0.3 ± 0.1. The worst improvements are achieved by the pair G2-D7 showing the highest performance in session three. Nevertheless, they also obtained an increase in the average pick accuracy of more than 10% in the last session with respect to the beginning of the training.

Control performance: Figure 3 illustrates the trajectories computed for a sample pair (G1-C7) throughout all sessions, wherein the target reached corresponds to the one prompted by the cue (i.e., correct trials). Notably, there is an observable enhancement in spatial exploration across sessions. In the initial session, the pair was able to reach only the most central target objects. While, in sessions two and three, they managed to reach four targets, and in the subsequent two sessions, they successfully reached all five targets. Figure 3b portrays the Fréchet distance [19] with respect to ideal trajectories, computed by averaging the trajectories of all the correct trials of every pair and every session for each target. This metric is calculated for both correct and erroneous trials, with the mean value computed for each session. Additionally, Table 2 outlines the average Fréchet distance for each session and pair. Except for the pair G2-D7, the subjects showed a reduced Fréchet distance of more than

Published by
Verlag der Technischen Universität Graz

10.3217/978-3-99161-014-4-063

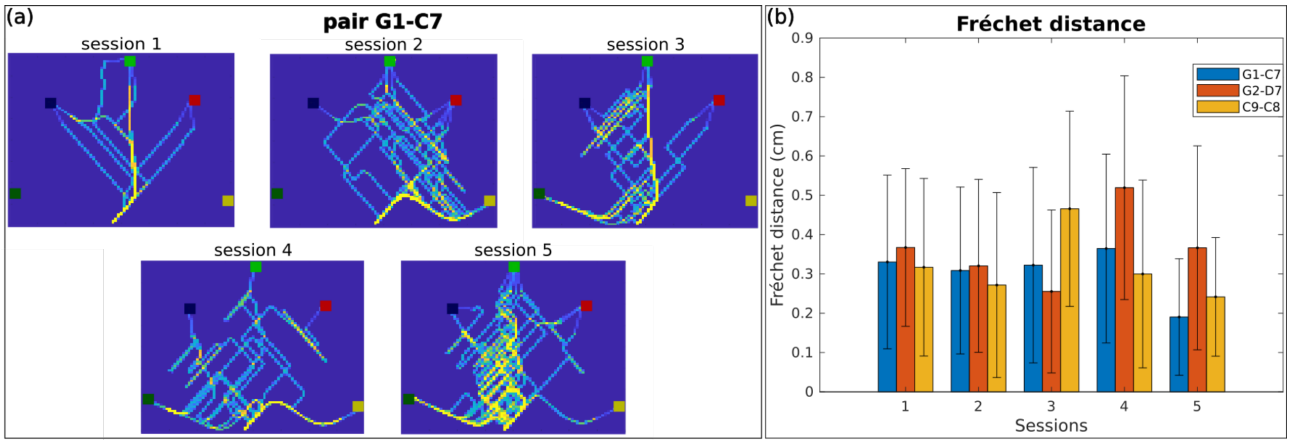

Figure 3: Control performances. (a) Correct trajectories computed by pair G1-C7 for each session. In the initial session, they reached three targets, while in the subsequent two sessions, they achieved four goals. Remarkably, in the last two sessions, they successfully reached all five targets. (b) Fréchet distance (in centimetres, cm) for each session and pair of subjects.

	G1-C7	G2-D7	C9-C8
session 1	33.0 ± 22.1	36.7 ± 20.0	31.6 ± 22.5
session 2	30.8 ± 21.2	32.0 ± 22.0	27.1 ± 23.5
session 3	32.2 ± 24.8	25.5 ± 20.7	46.5 ± 24.8
session 4	36.4 ± 24.0	51.9 ± 28.4	29.9 ± 23.8
session 5	19.0 ± 14.8	36.6 ± 25.9	24.1 ± 15.0

Table 2: Frechet distance (cm) for each session and pair.

$10cm$ in the last session with respect to the first session, signifying a reduced deviation of the paths traversed to the ideal trajectories.

DISCUSSION

As anticipated, the aim of this work is to deviate from the literature which uses the cBMI only as a method to increase the BMI performance but rather to exploit it in combination with a real robotic application as an innovative approach to foster the subject's learning. As reported in Figure 2, all the pairs show improvements in controlling the robotic device through the cBMI. Indeed, when the experiment started we hypothesised that each subject had a low capacity to control the robot, due to inexperience with this new approach, and because the modulation of brain rhythms is difficult at the beginning. More in details, at the beginning it was difficult for subject G1 to explore all the probability space of the BMI decoder. Nevertheless, thanks to the cBMI approach the pair was able to have sufficient control to directly train on the real robotic device and subject G1 learnt how to perform the required mental tasks leading to a more uniform distribution of the BMI output in the last sessions. It is worth noting that a broader spanning of the probability space is particularly important in our paradigm as the robotic device was controlled by mapping the BMI output to continuous control commands, rather than exploring a discrete control approach as commonly employed in the literature. By analysing the evolution of the neural correlates over the training sessions, we suggest that these improvements of performance in all the subjects are not only related to a familiarization of the subjects to the system, but rather to an effective learning of BMI skills. Indeed, the topographic maps of Figure 2(b) displays a visible increase in the number and power of the discriminant features in both α and β bands, in line with previous works on subject's learning in BMI [4, 5].

A thing to note is that the third session was done immediately after the winter holidays, thus more than two weeks apart from the previous two sessions. This may explain why all the pairs show a drop in the performance around the third and fourth sessions, as it can be seen also in Figure 2(c). Indeed, all the subjects were either completely naive or not proficient BMI users at the beginning of the experiment. Thus, they were not able to stabilize their features and skills in the short-term training before the stopping period. Nevertheless, when the training was restarted they recovered and further boosted the discriminant features. The learning of these BMI skills is also suggested by the performance of robot control. Two out of three pairs (G1-C7, C9-C8) showed an improvement in pick accuracy, pick error and Fréchet distance from the first to the last session, highlighting a more optimal control of the robotic manipulator directed to the desired target object.

Our study suggests that cBMI might be exploited as an alternative training protocol for MI BMIs. However, this work suffers from some limitations. First of all, the small number of subjects participating in the experiment, in fact, a larger pool is required to verify and strengthen our findings. Secondly, the relatively short training period (only 5 sessions) that might be not sufficient for all subjects to acquire stable and robust features. Future work will address these limitations by expanding the number of subjects and by designing a longitudinal study.

CONCLUSION

In this article, we introduce a novel protocol for collaborative MI BMI with shared control for manipulating a

Published by
Verlag der Technischen Universität Graz

10.3217/978-3-99161-014-4-063

robotic arm. Our hypothesis posited that with a collaborative BMI, both subjects would acquire proficiency in generating BMI commands and, thus, in controlling the robotic arm across multiple sessions. The outcomes obtained from a sample of three pairs of subjects, either completely naive or not expert in MI BMI, suggested promising results supporting our hypothesis and demonstrating the feasibility of utilizing this protocol to train subjects in acquiring BMI skills while directly engaging with real robotic application since the first days. We believe that the proposed approach of using the cBMI as training protocol will help not only to reduce the time investment required for reaching satisfying BMI performance, but also to mitigate the potential frustration experienced by naive users at the beginning of the training.

FUTURE WORKS

To further validate the proposed approach, we aim to evaluate in a larger study the improvements introduced by the collaborative BMI on the subject's learning with respect to training the subjects individually. Moreover, we want to investigate how the learning process is influenced by the pairing of individuals. Thus, we will compare the learning of pairs of both nave subjects with respect to pairing a naive subject with an expert BMI user. Finally, the use of the proposed cBMI will be extended to other and more challenging scenarios such as controlling the robotic arm in daily-living tasks or for entertainment in collaborative gaming applications.

ACKNOWLEDGMENT

The work is partially funded by the Piano Nazionale di Ripresa e Resilienza (PNRR), Project PE8 "AGE-IT" (Spoke 9) and Progetti di Rilevante Interesse Nazionale (PRIN 2022, 2022BCZ52A) - Ministero dell'Università e della Ricerca. This manuscript reflects only the authors' views and opinions, neither the European Union nor the European Commission can be considered responsible for them.

REFERENCES

[1] McFarland DJ, Wolpaw JR. EEG-based brain–computer interfaces. current opinion in Biomedical Engineering. 2017;4:194–200.
[2] Abiri R, Borhani S, Sellers EW, Jiang Y, Zhao X. A comprehensive review of EEG-based brain–computer interface paradigms. Journal of Neural Engineering. 2019;16(1):011001.
[3] Alimardani M, Nishio S, Ishiguro H. Brain-computer interface and motor imagery training: The role of visual feedback and embodiment. Evolving BCI Therapy-Engaging Brain State. Dynamics. 2018;2(64).
[4] Tortora S et al. Neural correlates of user learning during long-term BCI training for the cybathlon competition. Journal of NeuroEngineering and Rehabilitation. 2022;19(1):1–19.
[5] Tonin L et al. Learning to control a BMI-driven wheelchair for people with severe tetraplegia. iScience. 2022;25(12).
[6] Leeb R et al. Transferring brain–computer interfaces beyond the laboratory: Successful application control for motor-disabled users. Artificial intelligence in medicine. 2013;59(2):121–132.
[7] Poli R, Valeriani D, Cinel C. Collaborative brain-computer interface for aiding decision-making. PloS one. 2014;9(7):e102693.
[8] Bonnet L, Lotte F, Lécuyer A. Two brains, one game: Design and evaluation of a multiuser BCI video game based on motor imagery. IEEE Transactions on Computational Intelligence and AI in games. 2013;5(2):185–198.
[9] Valeriani D, Poli R, Cinel C. Enhancement of group perception via a collaborative brain–computer interface. IEEE Transactions on Biomedical Engineering. 2017;64(6):1238–1248.
[10] Yijie Z et al. A multiuser collaborative strategy for MI-BCI system. In: 2018 IEEE 23rd International Conference on Digital Signal Processing (DSP). 2018, 1–5.
[11] Wang Y, Wang YT, Jung TP, Gao X, Gao S. A collaborative brain-computer interface. In: 2011 4th International Conference on Biomedical Engineering and Informatics (BMEI). 2011, 580–583.
[12] Myrden A, Chau T. Effects of user mental state on EEG-BCI performance. Frontiers in human neuroscience. 2015;9:308.
[13] Roc A et al. A review of user training methods in brain computer interfaces based on mental tasks. Journal of Neural Engineering. 2021;18(1):011002.
[14] Müller-Putz G, Scherer R, Brunner C, Leeb R, Pfurtscheller G. Better than random: A closer look on bci results. International journal of bioelectromagnetism. 2008;10(1):52–55.
[15] Tortora S, Tonin L, Chisari C, Micera S, Menegatti E, Artoni F. Hybrid human-machine interface for gait decoding through bayesian fusion of EEG and EMG classifiers. Frontiers in Neurorobotics. 2020;14:582728.
[16] Lin TY, Goyal P, Girshick R, He K, Dollár P. Focal loss for dense object detection. In: Proceedings of the IEEE international conference on computer vision. 2017, 2980–2988.
[17] Tortora S, Gottardi A, Menegatti E, Tonin L. Continuous teleoperation of a robotic manipulator via brain-machine interface with shared control. In: 2022 IEEE 27th International Conference on Emerging Technologies and Factory Automation (ETFA). 2022, 1–8.
[18] Gottardi A, Tortora S, Tosello E, Menegatti E. Shared control in robot teleoperation with improved potential fields. IEEE Transactions on Human-Machine Systems. 2022;52(3):410–422.
[19] Alt H, Godau M. Computing the Fréchet distance between two polygonal curves. International Journal of Computational Geometry & Applications. 1995;5(01n02):75–91.

Published by
Verlag der Technischen Universität Graz